Impacts of Antarctic runoff changes on the Southern Ocean sea ice in an eddy-permitting sea ice-ocean model

Verena Haid[1], Dorotea Iovino[1] and Simona Masina[1,2]

[1]Ocean Dynamics and Data Assimilation, Centro Euro-Mediterraneo sui Cambiamenti Climatici, Bologna, 40128, Italy
5 [2]Istituto Nazionale di Geofisica e Vulcanologia (INGV), Bologna, 40128, Italy

Correspondence to: Verena Haid (v.haid@web.de)

Abstract. In a warming climate, observations indicate that the sea ice extent around Antarctica has increased over the last decades. One of the suggested explanations is the stabilizing effect of increased mass loss of the Antarctic ice sheet. We investigated the sea ice response to changes in the amount and especially the spatial distribution of freshwater. We
10 performed a sensitivity study by comparing a set of numerical simulations with additional supply of water at the Antarctic ocean surface. Here, we analyse the response of the sea ice cover and the on-shelf water column to variations in the amount and distribution of the prescribed surface freshwater flux.

Our results confirm that an increase in fresh water input can increase the sea ice extent. However, a very strong increase of freshwater will eventually invert the trend. Our experiments suggest that the spatial distribution of the freshwater is of great
15 influence. It affects sea ice dynamics and can strongly alter regional sea ice concentration and thickness. For strong regional contrasts in the freshwater addition the local change in sea ice is dominated by the dynamic response, which generally opposes the thermodynamic response. Furthermore, we find that additional coastal runoff generally leads to fresher and warmer dense shelf waters. Comparing our results with the observed trend, we estimate that the current increase of fresh water originating from the Antarctic Ice Sheet contributes between 5% and 24% to the trend observed in the sea ice extent.

20 ## 1 Introduction

In an environment of global warming, the sea ice extent in the Southern Ocean shows an increase in the satellite data collected since 1979. The positive circumpolar trend is the sum of partly opposing regional trends of the same order of magnitude (Parkinson and Cavalieri, 2012). Several mechanisms have been proposed to explain the expanding Antarctic sea ice. Many studies attribute the increase of sea ice to changes in the circumpolar wind field. The strengthening of the
25 circumpolar westerly winds alters the sea ice drift patterns and could result in the regionally different trends observed in the sea ice cover (e. g. Thompson and Solomon, 2002; Liu et al., 2004; Lefebvre and Goosse, 2005; Turner et al., 2009). An increase of precipitation over the Southern Ocean has influence on surface salinity, albedo of ice covered areas and ice thickness by submersion and could also be a possible contributor to the observed increase in Antarctic sea ice extent (Liu and Curry, 2010).

Zhang (2007) and Goosse and Zunz (2014) suggested that the trends in the Antarctic sea ice extent could be explained as the result of a feedback between the sea ice and the upper ocean stratification. Also Bintanja et al. (2013) attributes the change in sea ice to a fresher surface layer, but sees the cause in an enhanced Antarctic ice sheet melting.

5 The mass loss of Antarctic ice sheets by basal melt has recently been found to be accelerating (Jacobs et al., 2011; Pritchard et al., 2012) leading to the freshening of the mixed layer and thus to a stronger stratification of the water column. This shields the surface more effectively from the heat stored in the deeper layers of the ocean and therefore sea ice melt is reduced and sea ice growth is furthered. The importance of adding glacial melt water from the Antarctic continent to the Southern Ocean in simulations to account for ice-shelf melt water has been indicated by e.g. Hellmer (2004) and Stössel et al. (2007). However, so far, only few studies have been conducted to investigate the effect that changing Antarctic melt

10 water provokes in the Southern Ocean sea ice.

Bintanja et al. (2013) used a global coupled climate model to test the sensitivity of the Southern Ocean sea ice to an increase in Antarctic melt water and came to the conclusion that, while winds may be responsible for the regional trends, the circumpolar trend in sea ice is due to the increase of Antarctic melt water. With the CMIP5 ensemble Swart and Fyfe (2013) tested the influence of ice sheet melt on the sea ice area trends and concluded, that for realistic amounts of meltwater the

15 effects on the ice are small and that the freshwater addition is unlikely to reproduce the spatial pattern of the observed trends. More recently, Bintanja et al. (2015) simulated the impact of projected Antarctic mass loss on the future sea ice trends with a climate model and found that additional freshwater decelerates the negative ice area trend in the simulations and in high amounts can even invert it. Zunz and Goosse (2015) investigated the dependence of the forecasting skill of an Earth-system model on the freshwater input. Their results show a strong dependency on the initial state and in consequence they express

20 the opinion that neither atmospheric nor freshwater trends cause the current sea ice trends, but that the ocean's preconditioning of the 1970s lead to surface cooling and sea ice expansion.

These previous studies generally use very crude renderings of the spatial distribution of the freshwater addition. Our study aims to investigate the sensitivity of sea ice properties including the dynamic response to changes in the amount and especially the spatial distribution of fresh water input at surface. We focus on the differences between a widely-used uniform

25 runoff distribution around Antarctica and more complex spatially varying distributions. In our study, we employ an eddy-permitting ocean-sea ice model. Six experiments are carried out with differing spatial distribution and magnitude of the Antarctic freshwater flux at surface. Specifically, we study the response of sea ice concentration, thickness, velocity and production and deduce the development of sea ice extent and volume. The development of the on-shelf water column and the dense shelf water at the main sites of dense shelf water formation are presented, although the simulation period of 10 years is

30 too short for the water characteristics to reach equilibrium. While these changes do not directly correspond to the trends in sea ice extent observed around Antarctica in recent decades, they tell us how the sea ice reacts to spatially limited changes in the freshwater input and thus give us a measure of what to expect as a sea ice response to observed changes in the runoff and offer explanations for observed changes in sea ice and water properties.

2 Methods

2.1 Model description

The presented numerical calculations are based on version 3.4 of NEMO (Nucleus for European Modelling of the Ocean) global general circulation model (Madec et al., 2012). The ocean and sea ice components are run on a global ORCA tripolar

5   grid (an isotropic Mercator grid in the Southern Hemisphere, matched to a quasi-isotropic bipolar grid in the Northern Hemisphere with poles at 107°W and 73°E). The horizontal resolution is 0.25° (approximately 27.75 km) at the Equator and increases with latitude to be e.g. ≈10 km at 70°S (1442 grid points × 1021 grid points). The vertical grid has 75 levels the spacing of which increases with a double tanh function of depth from 1m near the surface to 205m at the bottom, with partial steps representing the bottom topography (Barnier et al., 2006).

10   The model bathymetry is based on the combination of ETOPO1 data set (Amante and Eakins, 2009) in the open ocean and GEBCO (IOC, IHO and BODC, 2003) in coastal regions. Hand editing is performed in a few key areas.

The ocean general circulation model OPA is a finite difference, hydrostatic, primitive equation ocean general circulation model and uses a linear free surface and an energy and enstrophy conserving momentum advection scheme. The horizontal viscosity is bi-Laplacian with a value of 1.8×10^{11} m^4 s^{-1} at the Equator, reducing poleward as the cube of the maximum grid

15   cell size. Tracer advection uses a total variance dissipation (TVD) scheme (Zalesak, 1979). Laplacian lateral tracer mixing is along isoneutral surfaces with a coefficient of 300 m^2 s^{-1}. The vertical mixing of tracers and momentum is parameterized using the turbulent kinetic energy (TKE) scheme. Subgrid-scale vertical mixing processes are represented by a background vertical eddy diffusivity of 1×10^{-5} m^2 s^{-1} and a globally constant background viscosity of 1×10^{-4} m^2 s^{-1}. The bottom friction is quadratic. A diffusive bottom boundary layer scheme is included.

20   The sea ice component is the Louvain-la-Neuve Sea Ice Model, LIM2 (Fichefet and Morales Maqueda, 1997), which includes the representation of both the thermodynamic and dynamic processes. It accounts for sensible heat storage within the ice. The vertical heat conduction is calculated assuming two layers of ice and a snow layer on top. Sub-grid scale thickness distributions are thereby accounted for by use of an effective conductivity. The model also includes the conversion of snow to ice if the ice surface is depressed under the sea surface by the snow load. The ice dynamics are calculated

25   according to external forcing from wind stress, ocean stress and sea surface tilt and internal ice stresses using C grid formulation (Bouillon et al., 2009). The elastic-viscous-plastic (EVP) formulation of ice dynamics by Hunke and Dukowicz (1997) is used.

The model is forced with ERA-Interim global atmospheric reanalysis (Dee et al., 2011), with 0.75°×0.75° spatial resolution. The turbulent variables are given as 3-hour mean values, while the radiative fluxes and precipitation are given as daily mean.

30   The surface boundary conditions are prescribed to the model using the CORE bulk formulation proposed by Large and Yeager (2004). The forcing routine and the ice model are called every 5 time steps of the ocean model (every 90 minutes).

A suite of simulations is presented in this manuscript: a control run (hereafter CTR) and five sensitivity experiments (S1-S5). CTR was started from a state of rest in January 1979 and run for 35 years. Initial conditions for temperature and salinity are

derived from the World Ocean Atlas 2013 climatological fields (Zweng et al., 2013; Locarnini et al., 2013), merged with PHC2.1 climatology over the Arctic region. The initial condition for the sea ice was inferred from the NSIDC Bootstrap products for January 1989. All freshwater experiments are branched off from CTR in January 2004 and run for ten years. In these simulations, we changed the amount and/or distribution of the Antarctic runoff; all other settings are identical to CTR.

5   The river run-off data is a monthly climatology from Dai and Trenberth (2002). It includes 109 major rivers and a coastal runoff and has a mean value of 1.26 Sv. The fresh water is added to the surface with zero salinity and at sea surface temperature. In the areas of freshwater addition, the vertical diffusion is enhanced (mixing coefficient: $2\times10\text{-}3$ m2 s-1) over a depth of 15 m. In the Southern Ocean, the runoff field is modified, as described in the next section. The runoff follows a seasonal cycle, which is unaltered relative to the mean amount in S1-S5 (Figure 1a).

10   No surface restoring for tracers was used in the simulations. The simulation was run without any constraint on the freshwater budget.

2.2 Experiment design

To test the response of sea ice to changes in the melting of glacial ice around Antarctica, we present five sensitivity experiments in this study, where the surface freshwater input is modified in its magnitude and spatial distribution. Ice shelves

15   and icebergs are not explicitly resolved in our configuration; therefore any source of melt water is represented in the runoff field.

The CTR total runoff represents a continental discharge of 2610 Gt yr^{-1}, and is uniformly distributed along the Antarctic coastline (Figure 1b), as commonly done in ocean models. The value is close to observation-based estimates of 2760 Gt yr^{-1} by Rignot et al. (2013), 2775 Gt yr^{-1} by Depoorter et al. (2013), and 2260 Gt yr^{-1} by Liu et al. (2015), that include both basal

20   melt and iceberg contributions. For information on the general performance of CTR please refer to the supplementary material.

In the first sensitivity experiment, S1, the magnitude of fresh water input is increased by 5% adding 130 Gt yr^{-1}, and is spatially constant as in CTR (Figure 1b). A comparison between the simulations allows us to study the effect of increased runoff without interference of other factors. The amount of increase is a conservative choice within the range of recent

25   estimations of Antarctic mass loss (e. g. Shepherd et al., 2012; Vaughan et al., 2013; Wouters et al., 2013; Velicogna et al., 2014).

S2 simulation introduces a more realistic uneven spatial distribution of the runoff based on estimates of basal melt and calving by Rignot et al. (2013). The runoff, still distributed close to the coastline, varies in magnitude by region (Figure 1c). In some areas (mainly East Antarctica), it is reduced compared to CTR, while in other areas (e.g. Weddell Sea and

30   Amundsen Sea) it is strongly increased. The total freshwater flux is increased by 150 Gt yr^{-1} compared to CTR.

S3 takes into account that not all the fresh water entering the ocean is added at the coastline. With a spatial distribution similar to S2, only a reduced amount of runoff (1670 Gt yr[-1)] is distributed close to the coastline to represent ice shelf melt. 1090 Gt yr^{-1} are widely distributed (with four levels of flux intensity) in the Southern Ocean to represent icebergs melting in

the open ocean (Figure 1d). The shape of this distribution is loosely based on iceberg drift and melt studies, e.g. Gladstone et al. (2001), Silva et al. (2006) and Jongma et al. (2008). The total amount of runoff is 2760 Gt yr^{-1} as in S2.

S4 features a more extreme distribution of runoff that focuses on the key areas of dense water formation. Since the sea ice formation processes over the Antarctic continental shelves are essential factors in the formation of dense shelf water and

5 consequently of the bottom water of the world ocean, the effect of runoff on the water column in these areas is of special interest. The S4 runoff adds 420 Gt yr^{-1} to the CTR runoff, but distributes it all in only three locations: in front of the Filchner/Ronne Ice Shelf in the Weddell Sea (230 Gt yr^{-1}), in front of the Ross Ice Shelf in the Ross Sea (120 Gt yr^{-1}) and in front of the Amery Ice Shelf in Prydz Bay (60 Gt yr^{-1}) (Figure 1e). The total of the runoff is 3030 Gt yr^{-1}.

S5 is designed to study the effect of the accelerated melting of Antarctic ice shelves. It starts with the freshwater distribution

10 of S2, but the runoff amount increases from 2760 Gt yr^{-1} in 2004 to 3310 Gt yr^{-1} in 2013 in 4 steps (137 Gt yr^{-1} every 2 years).

3 Sea ice

In this section, the impact of modifications in the freshwater supply on the sea ice is analyzed by comparing the sensitivity experiments with CTR. In the comparison, we focus on the austral winter period from April to September, since the sea ice

15 values in CTR are closest to observations during these months (see supplementary material for a detailed description of CTR results).

In Sect. 3.1, we analyse the resulting differences in sea ice concentration, thickness and velocity for all runoff scenarios and in Sect. 3.2 we discuss the time series of ice extent, volume and ice production. Our results regarding the sea ice properties are set in relation to previous model studies and observations in Sect. 3.3.

20 **3.1 Spatial response patterns**

Since sea ice concentration in CTR (Figure 2a) is already high during the winter months, there is only limited leeway for it to increase in the sensitivity runs. The maximum changes are found in the marginal ice zone (Figure 2, left column). The variability of the differences between scenarios S1-S5 and CTR is comparatively high, so areas with a high statistical confidence level are limited. Changes of the sea ice thickness (Figure 2, middle column) generally exhibit a similar, but

25 spatially more coherent pattern compared to the changes in sea ice concentration: areas of higher (lower) concentration yield thicker (thinner) sea ice. The longer-lasting character of the changes in thickness reduces the variability and increases the areas of statistical significance compared to the changes in concentration. Also the sea ice velocity is affected by the changes in runoff. The addition of fresh water affects the sea surface height (SSH). A change in the SSH slope influences the surface current of the ocean and the sea ice drift. Therefore, changes in the runoff scenario directly affect sea ice properties by both

30 thermodynamic and dynamic processes. The velocity of the sea ice is altered by changes in the fresh water input and in consequence affects the ice thickness due to dynamic compaction. The areas featuring a high statistical confidence level for

the changes in sea ice velocity (Figure 2, right column) are predominantly found along the coastline. Here, the runoff addition per area is highest in the sensitivity experiments and the coastal current distributes the added fresh water within a narrow band circling the continent. Most of the offshore velocities show seemingly erratic changes induced by the highly variable fronts and eddies in the Antarctic Circumpolar Current.

3.1.1 S1: Response to a simple runoff increase

In S1, the sea ice concentration features small changes from CTR, except for an increase at the tip of the Antarctic Peninsula (Figure 2d). Also the changes in ice thickness are small, but increases dominate in the western Ross Sea, west of and at the tip of the Antarctic Peninsula, and in the central Weddell Sea (Figure 2e). The main areas of sea ice thinning are the eastern Ross Sea and the southwestern Weddell Sea. The addition of freshwater, by decreasing the surface salinity, increases the freezing temperature and inhibits heat transport from below and is expected to increase the ice cover. However we have to consider the ice dynamics in order to explain local maxima and especially decreases in either concentration or thickness. In S1, the freshwater increase along the coastline strengthens the coastal current and the coastal sea ice drift is slightly sped up compared to CTR (Figure 2f). The faster ice drift leaves some areas with younger and thus thinner ice. In areas with a more complex coastline geometry, it causes stronger convergence and compaction of the ice, thus creating higher ice concentrations and thicker ice.

3.1.2 S2: Response to strong regional runoff variations

The runoff distribution used in S2 introduces regionally-varied coastal surface freshwater fluxes. The responses of the sea ice properties can therefore be expected to be strongly region-dependent. The sea ice concentration (Figure 2g) features changes of high statistical confidence in the coastal area. Increases in ice concentration and thickness (Figure 2h) occur in the eastern Weddell Sea, in the western Ross Sea, close to the coast of East Antarctica, and east of the tip of the Antarctic Peninsula. Areas of strongly reduced sea ice are located adjacent to the coast of the Amundsen and eastern Ross Seas and in the southern Weddell Sea. Since in S2, the freshwater input is varied regionally along the coastline also the ice drift velocities are altered dependent on the location (Figure 2i). Compared to CTR, the westward ice drift is accelerated along the coast of the Amundsen and Ross seas. From the Prydz Bay to the southern Weddell Sea it is slower than in CTR. From here, sea ice speeds up compared to CTR, moving northward along the Antarctic Peninsula, to slow down again on the western side of the peninsula toward the Bellingshausen Sea. In S2, the changes in sea ice velocity cause most of the local changes in sea ice concentration and thickness.

To investigate the mechanisms controlling regional sea ice behaviour in S2 in more detail, we subdivided the widely-used 5 regions of the Southern Ocean (e.g. Parkinson and Cavalieri, 2008, 2012) into 10 regions (Figure 1a). With the exception of the western and eastern Weddell regions, which both have a width of 40° in longitude, all regions span 35°. A northern limit was also employed, chosen individually for every region, in a way to include areas under the influence of the westward coastal current, while excluding most of the areas with eastward sea ice drift.

The compilation of the regional differences in runoff and sea ice characteristics between S2 and CTR (Table 2) confirms, that the regional thermodynamic response to an increase (decrease) of runoff is an increase (decrease) of sea ice production. Only the western Ross Sea region (WRoS) is an exception to this rule, because here the increase of the runoff along the southern coastline is exceeded by the reduction of runoff along the north-south directed western coastline (Figure 1b). For

5   the sea ice production, however, the southern coastline is of greater influence because of frequent polynya activity due to southerly winds.

The change in sea ice presence (concentration, thickness and volume) in most regions is contrary to the thermodynamic response. This is strong evidence that the impact on regional sea ice presence in S2 is determined by the response of the sea ice dynamics, and that regional thermodynamics play only a minor role. The differences in the sea ice velocities change the

10   regional import and export rates of sea ice. Therefore, given strong regional contrasts of the freshwater addition, the dynamic response decides the development of sea ice presence in the area. In the S2 experiment, two regions show a different behaviour: the Wilkes Land (WiL) and the Bellingshausen Sea (BeS) sectors (Table 2). Both feature an increase in runoff, sea ice production, sea ice concentration and thickness. In WiL, the coastal current is dominated by the larger scale situation; the strong acceleration experienced in the Amundsen and Ross Seas, is inverted while circling East Antarctica (Figure 2i).

15   WiL is the only East Antarctic region where fresh water input is increased compared to CTR, but in spite of this the coastal current is losing speed. Therefore, both thermodynamic and dynamic response favour increased sea ice presence in the region.

In the BeS sector, the coastal current is least pronounced and current speeds are lowest of all regions in CTR (Figure 2c). In S2, the current speeds are even weaker in this region (Figure 2i). Sea ice drift therefore is of low importance. BeS is the only

20   region where the local thermodynamic response dominates the change in sea ice presence seen in S2.

3.1.3 S3: Response to wide-spread runoff addition

S3 features a widespread increase in sea ice concentration and thickness compared to CTR (Figure 2j-k), which is caused by higher local sea ice production. The addition of freshwater, by decreasing the surface salinity, increases the freezing temperature and inhibits heat transport from below. Since in S3 only a part of the freshwater is added at the Antarctic

25   shoreline, the coastal runoff is decreased compared to CTR in most areas and the coastal current is decelerated (Figure 2l), with the maximum deceleration along the Princess Martha Coast, in the eastern Weddell Sea. Only from the Amundsen Sea to the Ross Ice Shelf front, we find coastal velocities accelerated compared to CTR. In the Amundsen Sea, the acceleration leads to a sea ice depletion, because the ice is younger and the export from the region is increased. In the western Ross Sea, the increased velocities (Figure 3) lead to thicker sea ice (Figure 2, middle column) due to enhanced accumulation and

30   compaction of the sea ice against the coastline in the southwestern corner of the Ross Sea. Additionally, a sea ice convergence is created by the contrast between the runoff addition at the southern and at the western coastline of the Ross Sea (Figure 1c) causing the ice drift to slow.

In the central and eastern Weddell Sea, the fresh water addition causes the ice to thickened thermodynamically in S3. In the western Weddell Sea, sea ice thickness is increased (Figure 2k), contrary to the ice concentration (Figure 2j). The increased sea ice presence over the northern part of the Weddell Gyre inhibits the northward export east of the Antarctic Peninsula (Figure 2l) and leads to dynamic compaction there.

3.1.4 S4: Response to regional runoff addition

In S4, the changes in the sea ice variables feature a pattern similar to the pattern of S1 (Figure 2m-o). The strongest increase of both ice concentrations and thickness occurs around the tip of the Antarctic Peninsula and in the western Ross Sea, since the strengthened coastal current leads to more dynamical compaction in these areas. A decrease of ice thickness is found to the southeast of the peninsula (Figure 2n), which can be attributed to the fact that the ice is younger. In S4, additionally a decrease of sea ice concentration occurs at the Filchner/Ronne Ice Shelf front (Figure 2m). Since the runoff addition is regional and confined to the fronts of the Filchner/Ronne, Ross and Amery ice shelves, the coastal ice velocities increase in the Weddell Sea (Figure 2o) and deplete the area of ice. In Prydz Bay, we find a similar acceleration and a local decrease of ice concentration. In the Ross Sea, the coastline geometry has a blocking effect.

3.1.5 S5: Response to runoff increase with time

S5 features a very similar spatial pattern of changes in sea ice concentration, thickness and velocity as S2 (Figure 2p-r), since the spatial distribution of runoff is the same and only the amount of freshwater is increased over time. In sea ice velocity, S5 differs from CTR as S2 does (Figure 2r), although the drift velocity along the coast is generally higher than in S2. This leads to the dynamical effects, like the thickening in the western Ross Sea or the depletion of sea ice in the Amundsen and the southern Weddell Seas, to increase compared to S2. However, in the offshore area of the eastern Weddell Sea the sea ice thickness and concentration are predominantly reduced instead of increased compared to CTR. A similar behaviour is evident in the offshore eastern Ross Sea for the sea ice thickness. The total of the sea ice cover is decreased compared to S2. The reasons lie in the surface warming of extensive areas and are discussed further in Sect. 3.2.

In summary, all scenarios confirm that the increase in drift velocity in areas of a strong contrast in freshwater addition prevails against local thermodynamic effects and lead to thinner sea ice in lower concentrations in the region. This is the expected case for the southern Weddell Sea and the Amundsen Sea, which are located downstream of areas where less runoff addition is expected. In regions downstream of high additional freshwater flux, the increased velocities can have the opposite effect on ice thickness, when encountering obstacles like headlands. The dynamic compression is enhanced and the sea ice increases in thickness. In the western Ross Sea, this effect is very efficient. It occurs also at other locations e.g. the tip of the Antarctic Peninsula.

3.2 Development in time and variability

In this section, we assess the time-dependency of the effects of the freshwater additions in the different experiments as well as their effect on the seasonal cycle of sea ice extent, volume and production. The time series of the sea ice variables over the course of the 10-year integration period are presented in Figure 3 with the addition of the mean seasonal cycles of the variables.

The differences in sea ice extent (Figure 3a-b) between all scenarios (S1-S5) and CTR are very small compared to the extent's seasonal amplitude (equal to 1.7×10^7 km^2). However, while the interannual and seasonal variability of the differences in ice extent is high, all scenarios result in a higher sea ice extent than CTR in the mean over the simulated period (Figure 3b). S1 diverges from CTR only to a small extent, and although the increase of ice extent prevails over the 10-year integration period, there are many occasions when S1 features a smaller sea ice extent than CTR. The magnitude of difference in ice extent between S2 and CTR is comparable with those of S1, but with distinct events of larger (smaller) ice extent in winter 2009-2011 (2012-2013).

S3 and S4 show a more substantial increase in sea ice extent. In S3, the widespread distribution of additional freshwater causes the sea ice to thermodynamically thicken and increases its concentration. In S4, the dominant factor is the dynamic compression due to more convergent ice drift. In both cases the increased ice thickness extends the ice's lifespan. Therefore, the sea ice extent is increased and most effectively during the austral summer.

S5 features similar results as S2, but in comparison it yields a smaller sea ice extent than S2 in the mean. The main contribution to this decrease comes from the eastern Weddell Sea and the Cosmonaut Sea, where S5 features thinner and less concentrated ice at the ice edge in connection with a higher sea surface temperature (SST).

As seen for sea ice extent, the differences of the sea ice volume between simulations and CTR (Figure 3c-d) are small compared to the volume's seasonal amplitude (1.4×10^4 km^3). The S1 ice volume is generally comparable to CTR from February to May, but tends to increased values from June to January. The S2/S5 differences to CTR in ice volume feature a larger interannual variability. During the first seven years the volume generally surpasses that of CTR, but drops to lower values during 2011 to return to an increasing trend in the last two years. In the 10-year mean, the seasonal cycle of S2 and S5 shows a larger volume than CTR, except in the late summer and early autumn. S3 produces higher sea ice volumes than CTR and all other scenarios through almost the entire simulated period, due to the widespread increase in both sea ice concentration and thickness. Similar to S2 and S5, the initial strong increase is interrupted in 2011 when a sudden drop in ice volume occurs, although the ice volume of S3 remains higher than in CTR. These experiments featuring a drop in ice volume in 2011 share a strongly regional distribution of runoff, indicating that the source also is regional, probably of atmospheric origin. The main contributing regions are the Amundsen, Bellinghausen and western Weddell Seas. S4, like S1, seems unaffected by the 2011 event and features distinctly increased ice volumes compared to CTR. The difference is comparatively small in the end of summer and reaches maximum values in spring.

Figures 3e-f show the changes in sea ice production caused by the runoff alterations. Again, the differences in sea ice production (Figure 3e) are small compared to the seasonal amplitude (1.6×10^6 m^3 s^{-1}) of the ice production. All scenarios feature a sea ice production larger than CTR from autumn to spring, but in contrast also the summer melting is higher in S1-S5 than in CTR. In S1, the changes are smallest and of a similar magnitude as their variability, while S3 diverges from CTR to the greatest extent and maintains a distinctly higher ice production even late in the year. While a strong stratification and a decoupled surface layer lead to cold surface waters and high ice production during the freezing period, in summer the heat uptake by the ocean is distributed in a shallower layer. Thus SST is higher and sea ice melt is enhanced. This behaviour is strengthened by a positive feedback loop as long as the ocean gains heat.

During autumn the sea ice production of S5 surpasses that of S2, since the lower surface salinity facilitates ice formation. However, during winter and spring S2 features higher values, because the influence of the offshore areas, particularly the northeastern Weddell and Ross Seas, becomes dominant. Once the fresher surface water has been advected offshore, the stronger stratification leads to a shallow surface layer. The heat uptake during the melting period therefore leads to higher temperatures, especially in the regions close to the winter ice edge. In S5, SST in the winter mean is higher than in S2 in the northeastern Weddell Sea and northeastern Ross Sea. Those higher temperatures are remnants of the summer heat uptake and lead to faster ice melt during winter. Another factor responsible for the difference between S2 and S5 is dynamics related. The increased speed of the coastal ice drift can affect the sea ice thickness twofold: it shortens the period of time available for thermal growth and it can strengthen the mechanical processes thickening the ice in areas of convergence. Depending on the regional geometry and the ice drift pattern, either the thermodynamic or the dynamic effect on the sea ice thickness prevails and leads to thinner or thicker sea ice, respectively. While in WRoS, the sea ice in S5 is thicker than in S2 due to compression against the shoreline, the thermodynamic effect is of greater influence in WWeS, where large areas feature thinner ice in S5 (Figure 2h and q).

3.3 Comparison with previous studies and observed trend

All sensitivity experiments have a higher amount of runoff compared to CTR that results in more sea ice. On a hemispheric scale, the experiments S1-S4 confirm the expectation that an increase in Antarctic runoff leads to an increase in sea ice in accordance with e.g. Bintanja et al. (2013) and Bintanja et al. (2015). However, comparing S2 and S5 shows that S5 (although with larger runoff) results in slightly less sea ice production, volume and extent. This suggests that there is a turning point (indeterminable from the experiments conducted for this study) in the sea ice response, where the amount of added freshwater exceeds the amount that leads to an increase in sea ice, and instead leads to a decrease.

The differences in runoff input applied in our simulations do not directly relate to the changes in Antarctic melt water estimated for the recent decades. An abrupt shift of freshwater sources from one region to another (as a comparison of CTR and S2 symbolizes) is unlikely, the increasing ocean temperatures are more likely to induce a slow but region-dependent increase of freshwater input. Similar to these natural processes is the difference between S2 and S5, where the (relative) spatial distribution of the Antarctic runoff does not differ, but the amount is increased. However, since the increase in S5 is

much faster than observed and the runoff amount surpasses current estimates of Antarctic mass loss (70-290 Gt yr^{-1}; Rignot et al., 2008; Joughin and Alley, 2011; Shepherd et al., 2012; Vaughan et al., 2013; Wouters et al., 2013; Rignot et al., 2013; Velicogna et al., 2014), a comparison with the recently observed hemispheric trend yields no similarities: S5 exceeds a turning point and results in less sea ice than S2. However, most regional trends are strengthened in S5 compared to S2 and

5   only in the eastern Weddell Sea and the Cosmonaut Sea regions the ice extent of S5 is closer to CTR than that of S2.

S1 and CTR also differ in amount of fresh water but not in its distribution. Although the runoff distribution in the two simulations is far from realistic, a comparison of our results with the observed sea ice trend is possible under some assumptions. Due to the abrupt runoff change in the simulations, a curve of the form $y \sim (a \times x)^b$ was fitted to the resulting differences in sea ice extent and projected for the duration of 35 years. For S1 (with a=0.0011 and b= 0.7469), this resulted

10   in an increase of the ice extent by 5.62×10^4 km^2 after 35 years due to 130 Gt yr^{-1} of additional Antarctic freshwater. Using the range of the available mass loss estimates (70-290 Gt yr^{-1}) and the observed change of 5.25×10^5 km^2 (15×10^3 km^2 yr^{-1}; Parkinson and Cavalieri, 2012), the simulated increase of sea ice extent in S1 corresponds to 5.8-23.9% of the observed increase (assuming a linear dependency on the runoff amount).

A similar comparison of the differences between S4 and CTR (with a=0.0086 and b=0.4165) yields 1.71×10^5 km^2 after 35

15   years. Considering the runoff addition (420 Gt yr^{-1}) in the simulation and the range of current estimates of Antarctic mass loss, we obtain a 5.4-22.5% runoff contribution to the currently observed trend in sea ice extent. Considering the differences in distribution of the additional fresh water between the experiments S1 and S4, the closeness of the obtained percentages gives the result some convincibility.

Like Swart and Fyfe (2013), we find the simulated trends in sea ice extent to be smaller than the observed trend for runoff

20   amounts close to observations and do not see the runoff as the main driving force of the circumpolar trend like Bintanja et al. (2013). However, we argue that the melt water increase currently contributes a roughly estimated 5-24% of the observed increase in sea ice extent and is thus not negligible.

We find the spatial distribution of the freshwater addition of high influence on the sea ice cover, as Zunz and Goosse (2015) suspected. In particular, considering an idealized freshwater discharge from icebergs strongly impacts sea ice thickness,

25   which in turn affects ice dynamics and longevity. Considering the effect that the spatial distribution of runoff has on sea ice, it seems important for modelling purposes to use a meltwater distribution as close to observations as possible. A readjustment of the sea ice parameters may be necessary to overcome the bias from tuning with a spatially unrealistic addition of freshwater.

Of course, in contrast to our idealized experiments, the fresh water from ice sheets and icebergs basal melt does not enter the

30   ocean only at the surface in the real world, but at tens or hundreds of meters depth. However, this approximation, still widely-used and to some extent imposed by the ocean model used, is applied in our study although we expect it to be of influence on the mean state and variability of the sea-ice. Also, this study neglects the heat fluxes associated with the melting of glacial ice.

4. On-shelf water characteristics

In this section, the influence of the different runoff scenarios on the on-shelf waters is presented for three locations, which are key regions for bottom water formation: the Weddell Sea, the Ross Sea and the Prydz Bay. The areas are limited for the Weddell Sea to west of 38° W and south of 71.7° S, for the Ross Sea to west of 170° W and south of 71.7° S and for Prydz

5   Bay to between 70° E and 80° E and south of 66.4° S. The regions are further limited to areas shallower than 550m depth to avoid strong influences from the deep ocean at the shelf break while including the outflow of dense water across the sills. Our comparison between S1-S5 and CTR focuses on the winter period (from April to September), when the dense shelf water is formed (Foldvik and Gammelsrød, 1988; Fahrbach et al., 1995).

In the mean vertical profiles of temperature, salinity and density computed in all three regions (Figure 4a-c, g-i, m-o), we

10 find a warming (cooling) of the waters at 300-500m depth corresponding to the freshening (salinification) of the upper water column. Strong spatial variations in freshwater addition may cause local deviations from this behaviour, due to advection. For example, in the Weddell Sea, despite the local strong addition of fresh water, S2 and S5 feature slightly saltier waters than CTR in the 100-300m depth interval, due to the preconditioning of the waters by the decreased runoff along the coastline of East Antarctica.

15 The evolution in time of the winter means of water properties at the 550m-isobath is presented for the simulated decade in Figure 4(d-f, j-l, p-r). The range of temperatures, salinities and densities at 550m depth between the simulations widens throughout the decade and the diverging trends can be expected to continue in subsequent years. The most extreme discrepancies of temperature and salinity in 2013 occur in the Ross Sea, where S5 features temperatures 1.4 K higher and salinities 0.09 psu higher than CTR. The highest discrepancy in density in 2013, however, occurs in the Weddell Sea, where

20 the water in S3 is 0.06 kg m^{-3} denser than in CTR.

In the Weddell Sea and in Prydz Bay, the S3 scenario mimicking an iceberg drift pattern yields much cooler and consequently also denser shelf waters. The surface salinity of S3 is increased compared to CTR in these locations and the water column is destabilized, because the coastal freshwater input is reduced in the region upstream (East Antarctica). Only in very few locations, the coastal freshwater input of S3 is larger than that of CTR (Figure 1). The most substantial increase

25 of runoff occurs in the Amundsen Sea area, which is upstream of the Ross Sea shelf. Therefore, in S3, we see a subsurface warming and increased stability of the water column compared to CTR in the Ross Sea.

Also S2 results in denser shelf waters than S5 in the Weddell Sea and in Prydz Bay, while in the Ross Sea, S5 creates denser water than S2. On the Ross Sea shelf, the density contrast between the surface and 500m depth is stronger than in the Weddell Sea or in Prydz Bay in our simulations. The waters at depths of 300-500 m are warmer and saltier than at the other

30 two locations due to warm water intruding upon the shelf (the simulation tends to overestimate warm water access due to its limited resolution of the bathymetry), and at the surface the salinity is lower due to the strong fresh water input in the Amundsen and Ross Seas. Therefore, the surface is decoupled more effectively from the sub-surface waters in the Ross Sea. The surface freshening does not translate to a freshening of the entire water column, but instead leads to increased sea ice

formation and eventually salt accumulation in the deeper water column. Thus, S5, the simulation with more freshwater input, creates the more saline and therefore denser shelf waters.

In contrast, S1 and S4 result in fresher shelf water than CTR in the Ross Sea. The freshening, however, mostly occurs in the last years of the simulated decade and is largely due to the destabilisation of the water column. Compared to CTR, S1 and S4

5   feature colder temperatures at 500m depth and higher salinities at the surface. Only S1 and S4 feature the same response in the dense shelf water in all three locations: temperatures are higher, salinities lower and densities decreased. In the Weddell and Ross Sea, S4 features the largest drop in salinity and consequentially density of all scenarios. In Prydz Bay, S2 and S5 feature a higher loss of salinity and density because here the water column is very unstable and the surface addition of fresh water easily translates to a freshening of the entire water column.

10 Our results regarding the formation of dense shelf water are in accordance with the findings of Hellmer (2004). Both studies support the idea that addition of fresh water leads to reduced density of the shelf waters, stronger stability of the water column and increased sea ice thickness (S1, S4). However, if aspects of spatially varying addition and subtraction of melt water come into play (as in S2, S3, S5), the processes become more complex and the preconditioning of the waters in upstream regions can cause results to differ locally.

15 **5. Conclusions**

To assess the impact of increased Antarctic freshwater fluxes at the surface on sea ice properties and dense water formation in the Southern Ocean, five simulations with varying freshwater forcing were performed and compared to the control run. We used the NEMO v3.4 ocean model coupled with the LIM2 sea ice model in a global configuration with horizontal resolution of 1/4°.

20 Our results confirm that the sea ice extent (and volume) increases for moderate increases of the runoff amount. The strongest freshwater forcing we used, however, leads to a decrease in sea ice volume and extent compared to other experiments. If the stratification of the offshore water column is increased, SST will increase during summer and lead to enhanced sea ice melting in winter, triggering a positive feedback loop. A freshwater-induced acceleration of the coastal current leads to thinner sea ice, when the time available for thermodynamical growth is reduced strongly. This is especially relevant for the

25 Weddell Sea, while in the western Ross Sea all performed experiments result in dynamically thickened sea ice.

For strong regional alterations of runoff addition, the dynamic response in our simulations proved to be stronger than the thermodynamic response in most cases. The region with additional runoff is depleted of sea ice since the coastal current is accelerated, and sea ice export from the region increases. The spatial distribution of freshwater addition is therefore of great importance.

30 Our results emphasize that the addition of freshwater induces a warming in the sub-surface waters due to the stronger stratification and the inhibited vertical heat exchange. On the continental shelves around Antarctica, the characteristics of the dense bottom waters are therefore subject to strong changes. In our experiments, the dense shelf water characteristics do not

reach an equilibrium within the 10-year simulation period, but it is evident that for simple increases in the runoff the dense shelf waters become warmer and fresher, and hence lose density. However, in regions downstream of reduced freshwater input at the coast, the water column is less stable and in consequence waters generated on the shelf are denser (colder and more saline).

5   We conclude that the increase of Antarctic melt water currently contributes to the positive trend in sea ice extent, but rough calculations limit its role to 5-24% of the observed increase. Changes in the runoff regional distribution can also induce regional variations in sea ice, as e.g. occurs in the Amundsen Sea, where the strong basal melt processes effectively reduce the sea ice cover and export more sea ice to the eastern Ross Sea. Generally, our experiments suggest that the spatial distribution of runoff around the Antarctic continent is of high importance for the sea ice cover and the stratification of the

10   Southern Ocean. Numerical applications may highly benefit from realistic distributions of Antarctic runoff.

It is worth noting that the impact on shelf water properties, simulated in our experiments, is due to fresh water, that enters the ocean only through the surface. These results may change with the additional water distributed at non-zero depth, for better representing calving and basal melting of the ice shelves. The freshening of underlying layers would decrease stability and impact the mixed layer depth. Also the influence of the heat fluxes associated with melting the glacial ice has not been

15   considered in this study.

Acknowledgments

This study was performed in the framework of Climatically driven changes of Antarctic sea ice and their role in the climate

20   system (CATARSI) project as part of the Italian National Program for Research in Antarctica (PNRA). The financial support of the Italian Ministry of Education, University and Research, and Ministry for Environment, Land and Sea (also through the project GEMINA) is gratefully acknowledged.

References

Amante, C. and Eakins, B. W.: ETOPO1 1 Arc-Minute Global Relief Model: Procedures, Data Sources and Analysis,

25   NOAA Technical Memorandum NESDIS NGDC-24, 19 pp., 2009.

Barnier, B., Madec, G., Penduff, T., Molines, J.-M., Treguier, A.-M., Le Sommer, J., Beckmann, A., Biastoch, A., Böning, C., Dengg, J., Derval, C., Durand, E., Gulev, S., Remy, E., Talandier, C., Theeten, S., Maltrud, M., McClean, J., and De Cuevas, B.: Impact of partial steps and momentum advection schemes in a global ocean circulation model at eddy-permitting resolution, Ocean Dyn., 56, 543–567, 2006.

Bintanja, R., van Oldenborgh, G. J., Drijfhout, S. S., Wouters, B., and Katsman, C. A.: Important role for ocean warming and increased ice-shelf melt in Antarctic sea-ice expansion. Nature Geoscience, 6(5), 376-379, 2013.

Bintanja, R., van Oldenborgh, G. J., and Katsman, C. A.: The effect of increased fresh water from Antarctic ice shelves on future trends in Antarctic sea ice, Ann. of Glaciology, 56(69), 120-126, 2015.

5 Bouillon. S., Morales Maqueda, M. A., Legat, V., and Fichefet, T.: An elastic-viscousplastic sea ice model formulated on Arakawa B and C grids, Ocean Modelling, 27:174–184, 2009.

Dai, A. and Trenberth, K. E.: Estimates of freshwater discharge from continents: Latitudinal and seasonal variations. J. Hydrometeorol., 3, 660-687, 2002.

Dee, D. P. et al., The ERA-Interim reanalysis: Configuration and performance of the data assimilation system. Q. J. R.
10 Meteorol. Soc., 137, 553–597, 2011.

Depoorter, M. A., Bamber, J. L., Griggs, J. A., Lenaerts, J. T. M., Ligtenberg, S. R. M., van den Broeke, M. R., and Moholdt, G.: Calving fluxes and basal melt rates of Antarctic ice shelves. Nature 502, 89-92, 2013.

Fichefet, T. and Morales Maqueda, M. A.: Sensitivity of a global sea ice model to the treatment of ice thermodynamics and dynamics, J. Geophys. Res., 102:12609–12646, 1997.

15 Gladstone, R. M., Bigg, G. R., and Nicholls, K. W.: Iceberg trajectory modelling and meltwater injection in the Southern Ocean, Journal of Geophysical Research, 106, C9, 19903-19915, 2001.

Goosse, H. and Zunz, V.: Decadal trends in the Antarctic sea ice extent ultimately controlled by ice–ocean feedback, The Cryosphere, 8, 453-470, 2014.

Hellmer, H. H., 2004: Impact of Antarctic ice shelf basal melting on sea ice and deep ocean properties, Geophys. Res. Lett.,
20 31, L10307.

Hunke, E. C. and Dukowicz. J. K.: An elastic–viscous–plastic model for sea ice dynamics, J. Phys. Oceanography, 27:1849–1867, 1997.

IOC, IHO, and BODC: Centenary Edition of the GEBCO Digital Atlas, published on CD-ROM on behalf of the Intergovernmental Oceanographic Commission and the International Hydrographic Organization as part of the General
25 Bathymetric Chart of the Oceans, British Oceanographic Data Centre, Liverpool, UK, 2003.

Jacobs, S. S., Jenkins, A., Giulivi, C. F., and Dutrieux, P.: Stronger ocean circulation and increased melting under Pine Island Glacier ice shelf, Nature Geoscience, 4(8), 519-523, 2011.

Jongma, J. I., Driesschaert, E., Fichefet, T., Goosse, H., and Renssen, H.: The effect of dynamic–thermodynamic icebergs on the Southern Ocean climate in a three-dimensional model. Ocean Modelling, 26, 104-113, 2008.

30 Joughin, I. and Alley, R. B.: Stability of the West Antarctic ice sheet in a warming world, Nature Geoscience, 4, 506–513, 2011.

Large, W.G. and Yeager, S.G.: Diurnal to decadal global forcing for ocean and seaice models: the data sets and flux climatologies, Technical Report NCAR/TN460+ STR, CGD Division of the National Centre for Atmospheric Research (NCAR) , 2004.

Lefebvre, W. and Goosse, H.: Influence of the Southern Annular Mode on the sea ice-ocean system: The role of the thermal and mechanical forcing, Ocean Sci., 1, 145–157, 2005.

Liu. J. and Curry, J. A.: Accelerated warming of the Southern Ocean and its impacts on the hydrological cycle and sea ice. Proc. Natl Acad. Sci. USA (PNAS), 107(34), 14 987–14 992, 2010.

5   Liu, J., Curry, J. A., and Martinson, D. G.: Interpretation of recent Antarctic sea ice variability, Geophys. Res. Lett. 31, L02205, 2004.

Liu, Y., Moore, J. C., Cheng, X., Gladstone, R. M., Bassis, J. N., Liu, H., Wen, J., and Hui, F.: Ocean-driven thinning enhances iceberg calving and retreat of Antarctic ice shelves, PNAS, 112, 11, 3263-3268, 2015.

Locarnini, R. A., Mishonov, A. V., Antonov, J. I., Boyer, T. P., Garcia, H. E., Baranova, O. K., Zweng, M. M., Paver, C. R.,

10   Reagan, J. R., Johnson, D. R., Hamilton, M., and Seidov, D.: World Ocean Atlas 2013, Volume 1: Temperature, S. Levitus, Ed., A. Mishonov Technical Ed.; NOAA Atlas NESDIS 73 , Silver Spring, MD, 40 pp., 2013.

Madec, G., and the NEMO team: Nemo ocean engine – Version 3.4. Technical Report ISSN No 1288–1619, Pole de modelisation de l'Institut PierreSimon Laplace No 27, 2012.

Parkinson, C. L. and Cavalieri, D. J.: Antarctic sea ice variability and trends, 1979–2010. The Cryosphere, 6, 871-880, 2012.

15   Pritchard, H. D., Ligtenberg, S. R. M., Fricker, H. A., Vaughan, D. G., van den Broeke, M. R., and Padman, L.: Antarctic ice-sheet loss driven by basal melting of ice shelves, Nature, 484, 7395, 502-505, 2012.

Rignot, E., Bamber, J. L., van den Broeke, M. R., Davis, C., Li, Y., van de Berg, W. J., and van Meijgaard, E.: Recent Antarctic ice mass loss from radar interferometry and regional climate modelling, Nature Geosci, 1, 106-110, 2008.

Rignot, E., Jacobs, S., Mouginot, J. and Scheuchl, B.: Ice-shelf melting around Antarctica, Science, 341, 6143, 266-270,

20   2013.

Shepherd, A. et al.: A reconciled estimate of ice-sheet mass balance, Science, 338, 1183-1189, 2012.

Silva, T. A. M., Bigg, G. R., and Nicholls, K. W.: Contribution of giant icebergs to the Southern Ocean freshwater flux, Journal of Geophysical Research, 111, C03004, 2006.

Stössel, A., Stössel, M. M., and Kim, J.-T.: High-resolution sea ice in long-term global ocean GCM integrations, Ocean

25   Modell., 16, 206–223, 2007.

Swart, N. C. and Fyfe, J. C.: The influence of recent Antarctic ice sheet retreat on simulated sea ice area trends, Geophysical Research Letters, 40(16), 4328-4332, 2013.

Thompson, D. W. J. and Solomon, S.: Interpretation of recent Southern Hemisphere climate change, Science, 296, 895-899, 2002.

30   Turner, J., Comiso, J. C., Marshall, G. J., Lachlan-Cope, T. A., Bracegirdle, T., Maksym, T., Meredith, M., Wang, Z., and Orr, A.: Non-annular atmospheric circulation change induced by stratospheric ozone depletion and its role in the recent increase of Antarctic sea ice extent, Geophys. Res. Lett., 36, L08502, 2009.

Vaughan, D. G. et al.: Observations: Cryosphere, in Climate Change 2013: The Physical Science Basis, Contribution of Working Group I to the Fifth Assessment Report of the Intergovernmental Panel on Climate Change, edited by T. F. Stocker et al., Cambridge Univ. Press, Cambridge, U. K, 2013.

Velicogna, I., Sutterley, T. C., and van den Broeke, M. R.: Regional acceleration in ice mass loss from Greenland and Antarctica using GRACE time-variable gravity data. J. Geophys. Res. Space Physics, 119, 8130–8137, 2014.

Wouters, B., Bamber, J. L., van den Broeke, M. R., Lenaerts, J. T. M., and Sasgen, I.: Limits in detecting acceleration of ice sheet mass loss due to climate variability, Nature Geosci., 6, 8, 613-616, 2013.

Zalesak, S.T.: Fully multidimensional flux-corrected transport algorithms for fluids, J. Comp. Physics, 31, 335-362, 1979.

Zhang, J.: Increasing Antarctic sea ice under warming atmospheric and oceanic conditions, J. Climate, 20, 2515-2529, 2007.

Zunz, V. and Goosse, H.: Influence of freshwater input on the skill of decadal forecast of sea ice in the Southern Ocean, The Cryosphere, 9, 541-556, 2015.

Zweng, M. M., Reagan, J. R., Antonov, J. I., Locarnini, R. A., Mishonov, A. V., Boyer, T. P., Garcia, H. E., Baranova, O. K., Johnson, D. R., Seidov, D., and Biddle, M. M.: World Ocean Atlas 2013, Volume 2: Salinity, S. Levitus, Ed., A. Mishonov Technical Ed.; NOAA Atlas NESDIS 74 , Silver Spring, MD, 39 pp. , 2013.
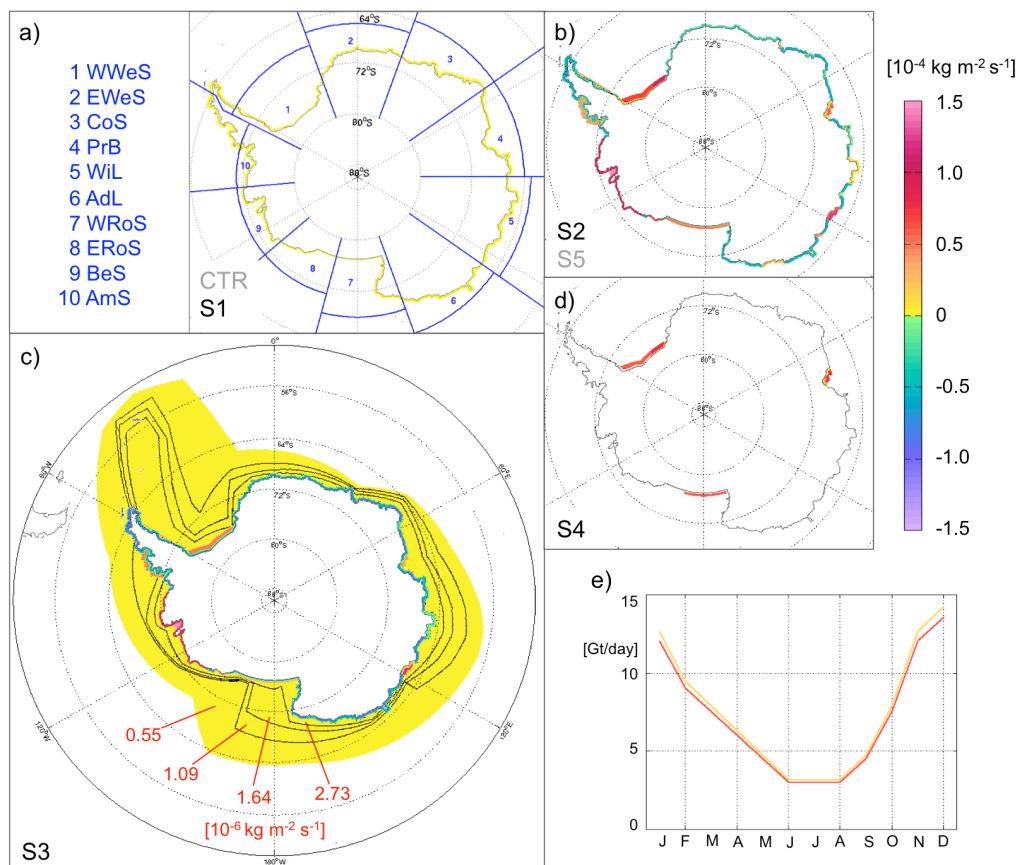
Figure 1: a) Seasonal cycle of the runoff, exemplary for CTR (red) and S1 (yellow); b-e) Runoff distributions for the scenarios as differences from the CTR runoff. The numbers vary with the seasonal cycle; shown is the mean for the winter half of the year (April-September). CTR (S5) has a similar distribution to S1 (S2) but different values.
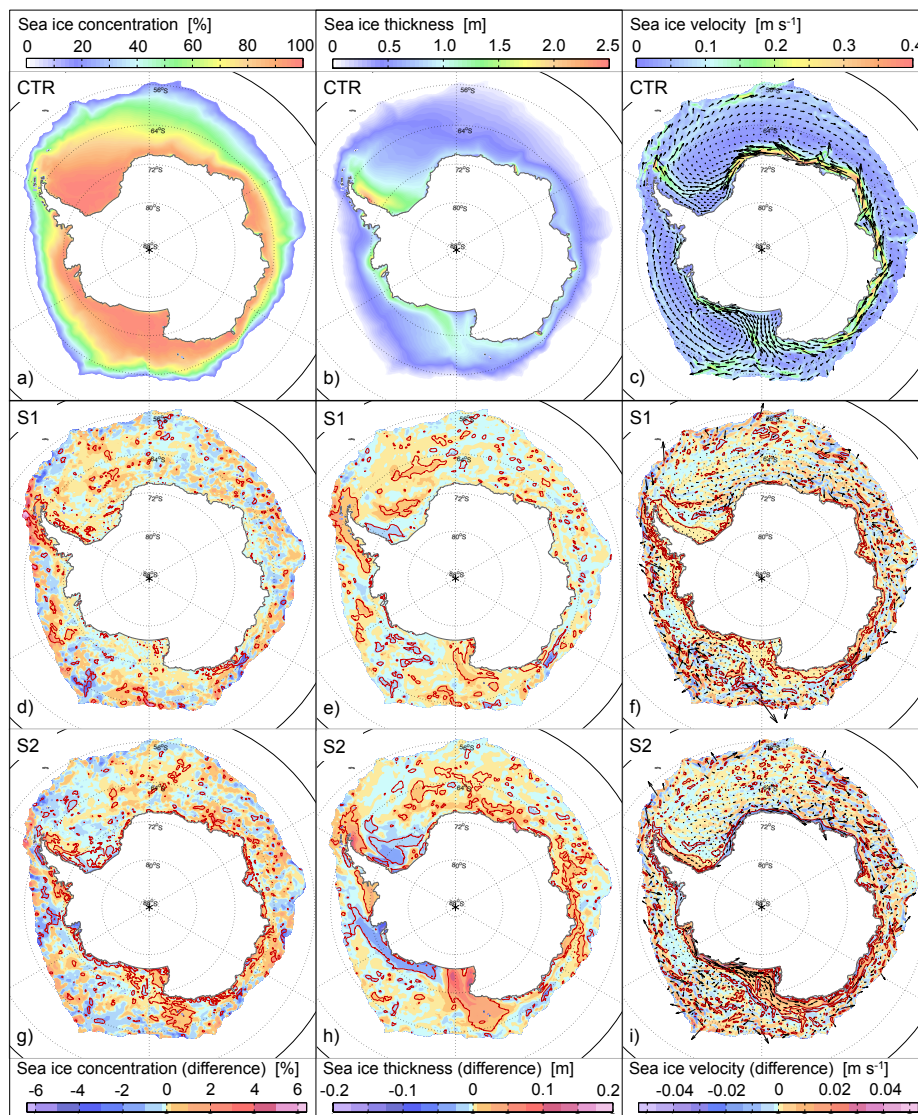
Figure 2: Maps of a) winter sea ice concentration, b) thickness, and c) velocity in CTR averaged over the years 2004-2013. b-r) Difference of ice concentration (left), thickness (middle), and velocity (right) between respective scenario and CTR. Dark red contours encompass the areas where the significance of the difference surpasses the 99% confidence-level of the Student t-test for dependent samples.
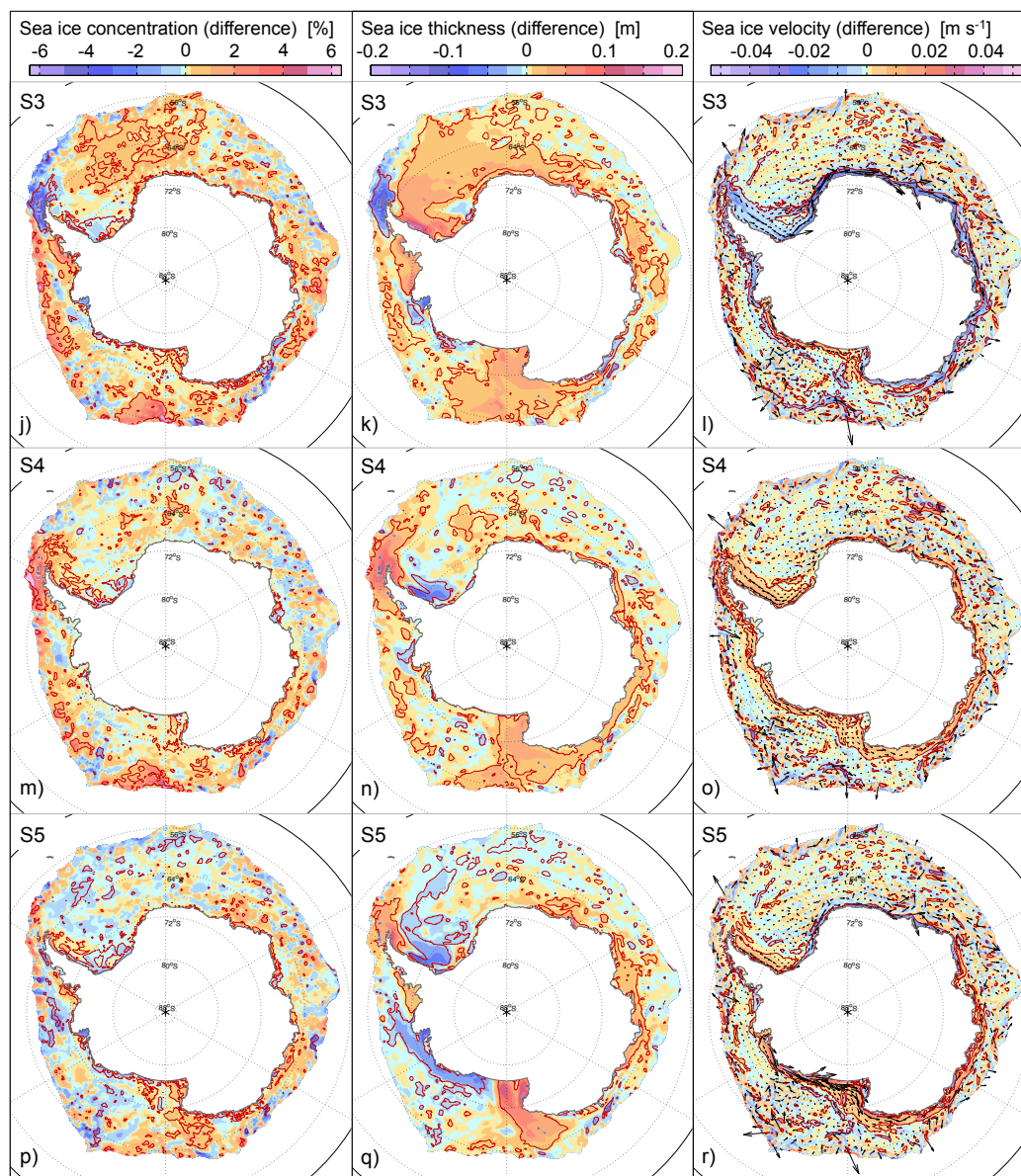
Figure 2 (continued).
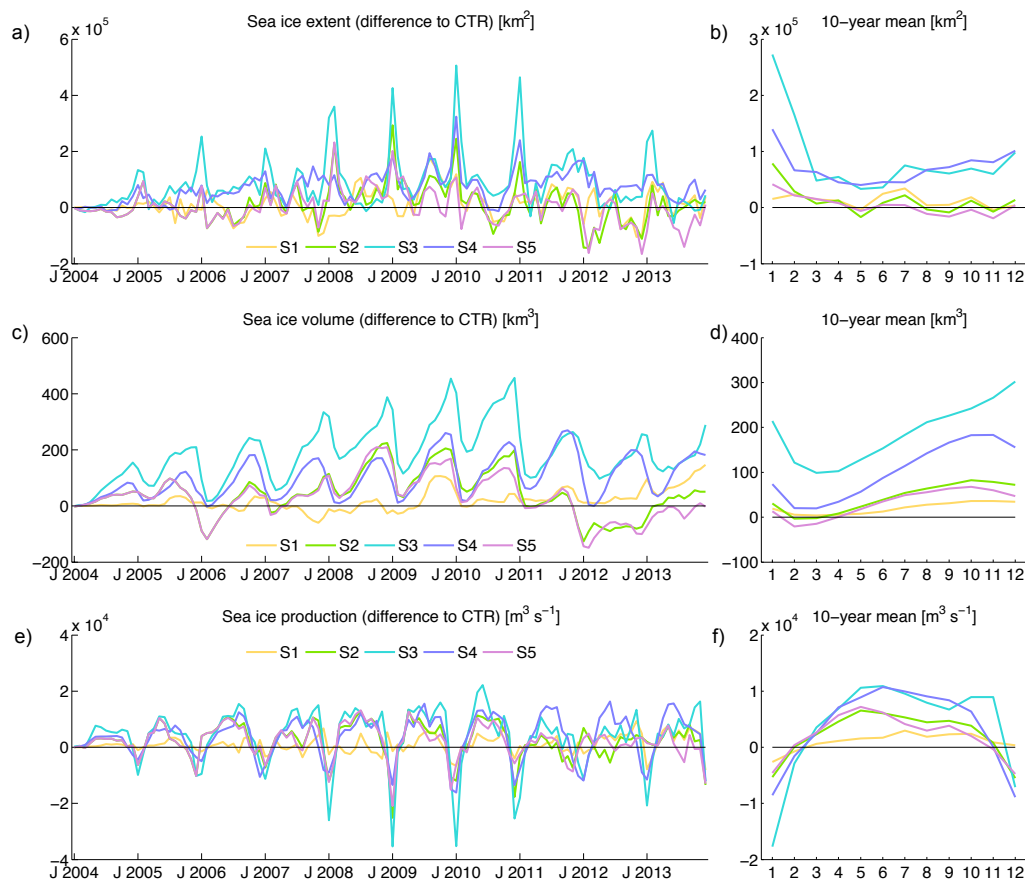
Figure 3: Time series of the differences of (a-b) sea ice extent, (c-d) sea ice volume and (e-f) sea ice production between respective scenario and CTR, monthly values for 2004-2013 (left column), monthly values averaged over the 10-year period (right column).
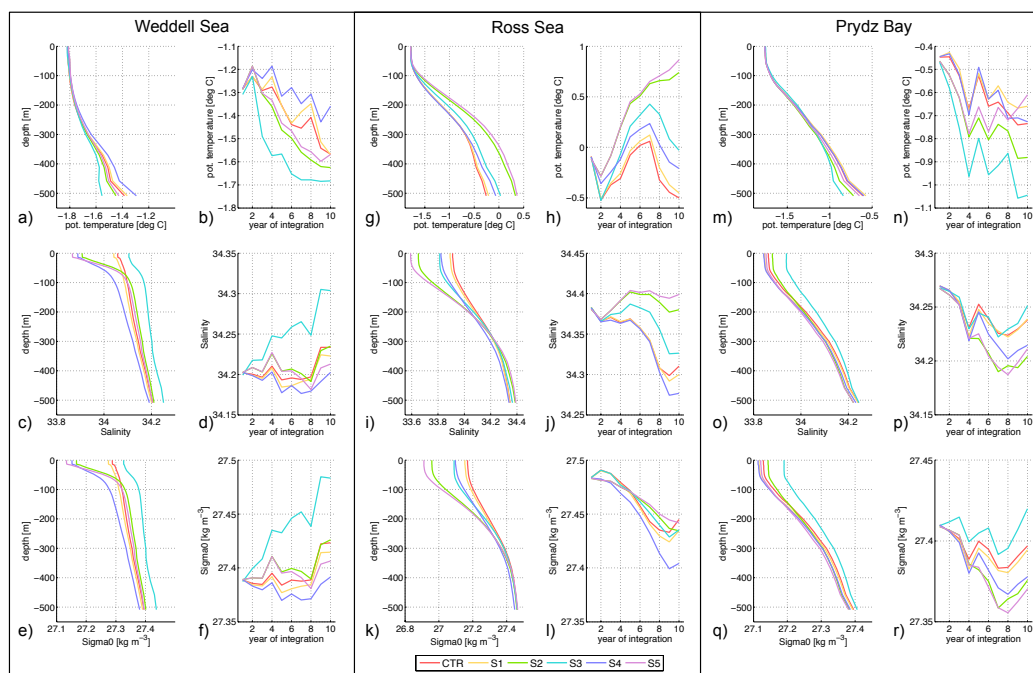
Figure 4. Mean vertical profile ≤550 m depth (left) and annual mean values at the 550m isobath (right) of potential temperature, salinity and sigma0 in April-September in the a-f) Weddell Sea, g-l) Ross Sea and m-r) Prydz Bay.

Table 1: Main features of the experiments.

Simulation	Runoff amount [Gt yr^{-1}]	Runoff distribution
CTR	2610	Uniform, coastal
S1	2740	Uniform, coastal
S2	2760	Regional, coastal
S3	2760	Regional, including offshore distribution
S4	3030	Additional coastal runoff at major ice shelves
S5	2760-3030	Regional, coastal, increasing in 4 steps

Table 2. Differences between S2 and CTR computed as winter mean over the selected regions for the 2004-2013 period. Positive numbers are printed in bold font.

Region	Runoff [Mt]	Ice production [km³ d⁻¹]	Ice concentration [%]	Ice thickness [cm]	Ice volume [km³]
West. Weddell Sea (WWeS)	**30**	**0.17**	-0.1	-1.0	-14
East. Weddell Sea (EWeS)	-8.4	-0.07	**0.04**	**0.6**	**5.0**
Cosmonaut Sea (CoS)	-16	-0.05	**0.3**	**1.1**	**6.8**
Prydz Bay (PrB)	-8.1	-0.005	**0.04**	**0.6**	**4.2**
Wilkes Land (WiL)	**1.1**	**0.02**	**0.02**	**0.8**	**4.0**
Adelie Land (AdL)	-13	-0.06	-0.06	**0.3**	**2.0**
West. Ross Sea (WRoS)	-0.84	**0.24**	**0.17**	**3.7**	**37**
East. Ross Sea (ERoS)	**8.4**	**0.15**	-0.16	-1.6	-10
Amundsen Sea (AmS)	**42.7**	**0.15**	-0.34	-3.3	-11
Bellingshausen Sea (BeS)	**0.9**	**0.016**	**0.29**	**1.8**	**2.8**